Supplementary Materials for
A Ultrafast self-healing and self-adhesive polysiloxane towards reconfigurable on-skin electronics

Miao Tang,[1] Zili Li,[2] Kaiqing Wang,[1] Yizhou Jiang,[2] Mi Tian,[3] Yajie Qin,[2] Ye Gong,[3] Zhuo Li[1], Limin Wu[1]**

[1]Department of Materials Science and State Key Laboratory of Molecular Engineering of Polymers, Fudan University, Shanghai 200433, China

[2]School of Information Science and Technology, Fudan University, 220 Handan Road, Shanghai, 200433, China

[3]Department of Critical Care Medicine, Department of Neurosurgery, Huashan Hospital, Fudan University, 12 Middle Wulumuqi, Shanghai, 200040, China.

*Corresponding author. E-mail: zhuo_li@fudan.edu.cn (Z. L.), lmw@fudan.edu.cn (L. W.)

Materials

Vinyl-terminated polydimethylsiloxanes (named v-$PDMS_1$ and v-$PDMS_2$) with molecular weight of 4064 g/mol and 8199 g/mol were purchased from the J&K, vinyl terminate polydimethylsiloxane (named v-$PDMS_3$) with molecular weight of 12440 g/mol was purchased from Sigma-Aldrich Company. Dithiothreitol (DTT) and a, a-dimethoxy-a-phenylacetophenone were purchased from the Aladdin Company. Boric acid (BA) was purchased from Sinopharm Chemical Reagent Co., Ltd., and grinded, sieved via a 100-mesh sieve aluminum screen and dried for 24 h before used. Silver nanowires (30 nm in diameter and 30 μm in length) were purchased from Zhejiang

Kechuang Advanced Materials Technology. Silver micro-flakes (SF-01C, 2~7 μm in diameter and 100~150 nm in thickness) were obtained from Sichuan Zhongchai Great Wall Precious Metal Co. Ltd. PDMS Sylgard 184 was obtained from Dow corning. All other chemicals were analytical grade reagents and used directly without further purification.

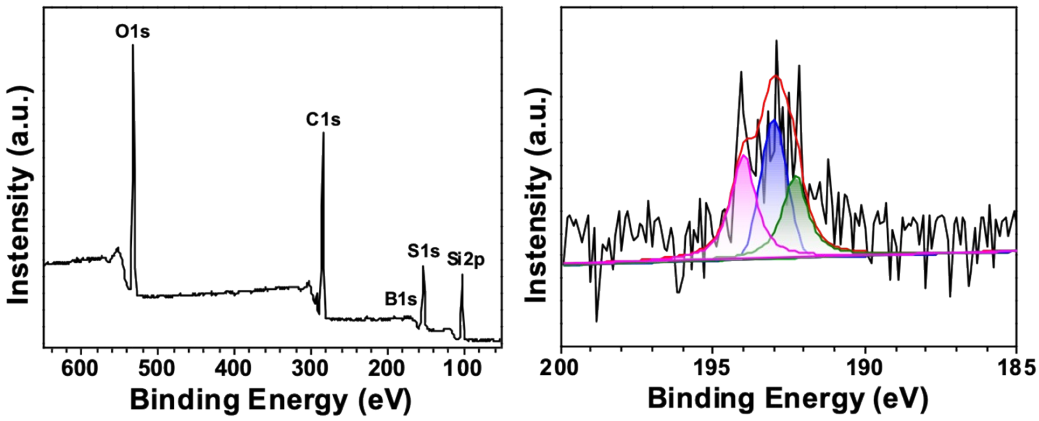

Figure S1. XPS survey spectrum (left) and the high resolution B1s spectrum (right) of the block PBS_1.

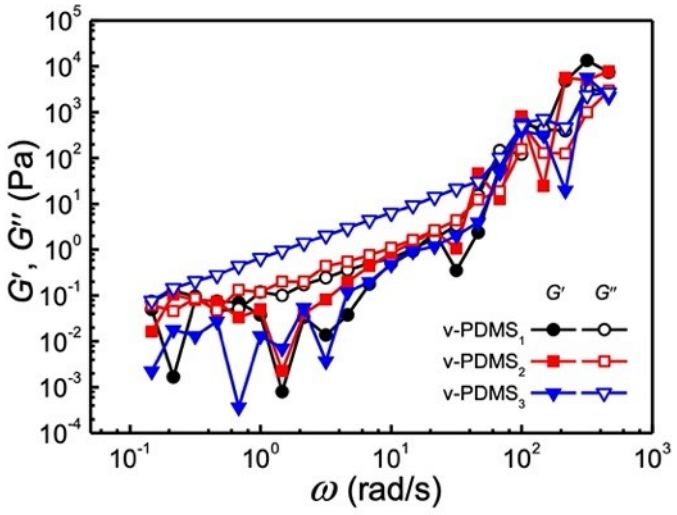

Figure S2. The storage (G') and loss (G'') moduli are recorded as a function of frequency (ω). G' and G'' of v-$PDMS_1$, v-$PDMS_2$ and v-$PDMS_3$.

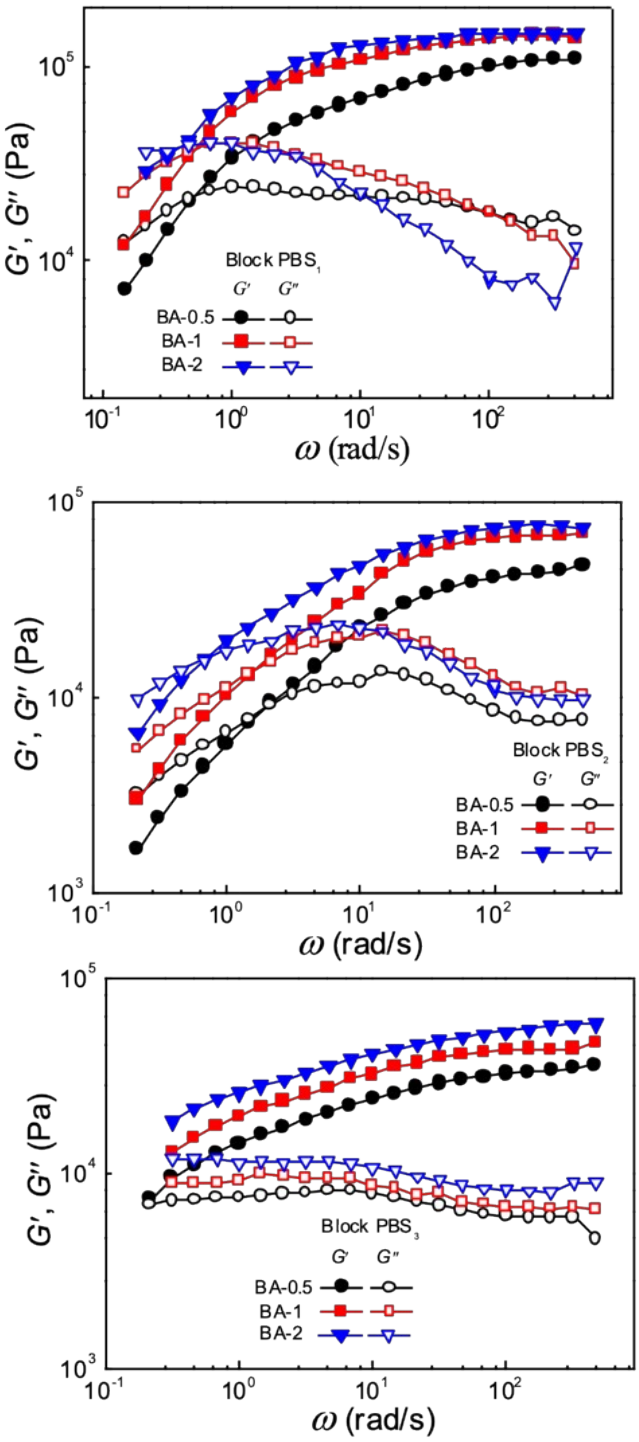

Figure S3. The storage (G') and loss (G'') moduli are recorded as a function of frequency (ω). G' and G'' of block $PBS_{1\text{-}3}$ prepared with different molar ratio of BA to block PDMS precursors**.**

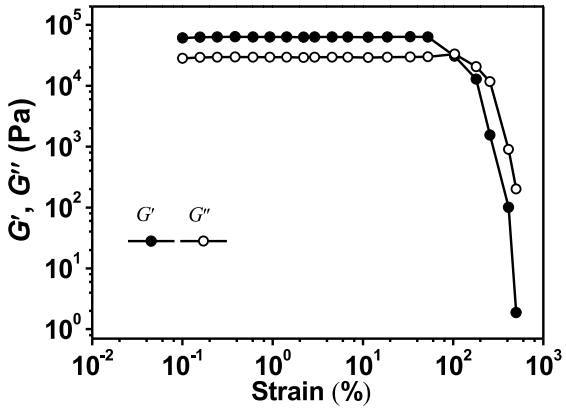

Figure S4. G' and G'' of block PBS under strain sweep at an angular frequency of 1.0 Hz.

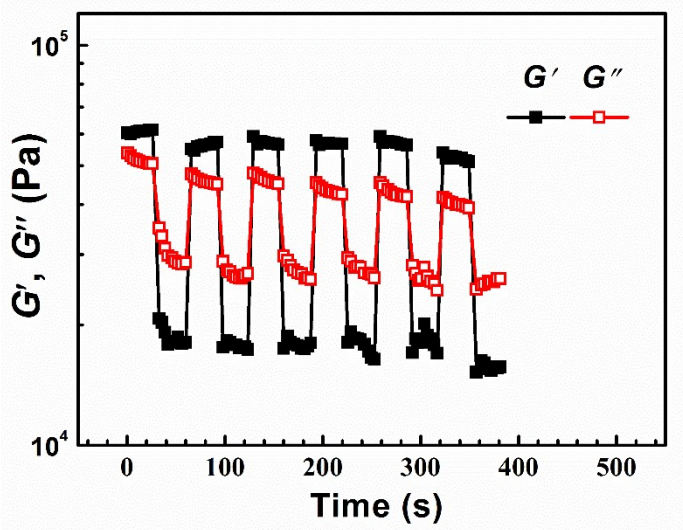

Figure S5. G' and G'' of block PBS under continuous strain sweep with alternate small oscillation force (1% strain) and a large one (500% strain) at an angular frequency of 1.0 Hz.

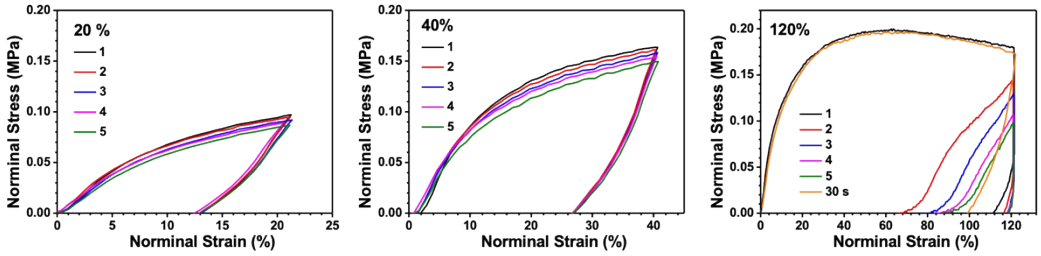

Figure S6. Cyclic stress-strain curves of block PBS_1 with different strain. The strain rate is 50 mm/min.

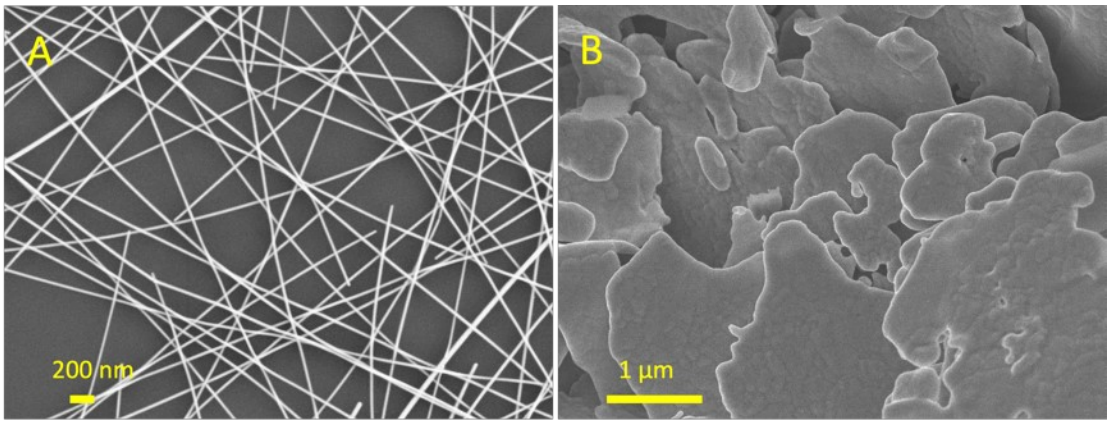

Figure S7. SEM images of conductive fillers. a, AgNWs. b, Ethanol treated silver flakes.

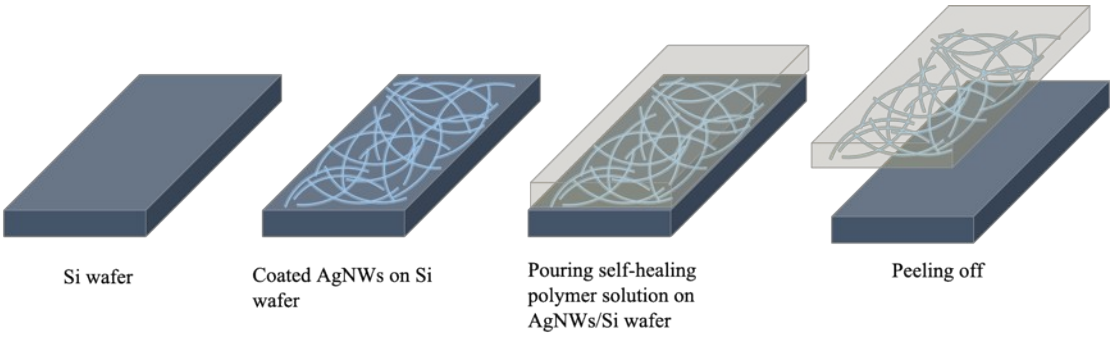

Figure S8. Schematic illustration of the fabrication process for the self-healable stretchable electrode by embedding AgNWs conductive network into self-healing polymer matrix.

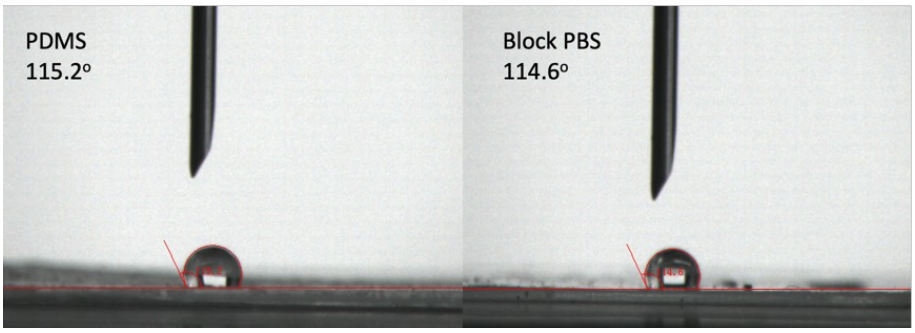

Figure S9. Contact angles of water droplets on PDMS and block PBS film surfaces.

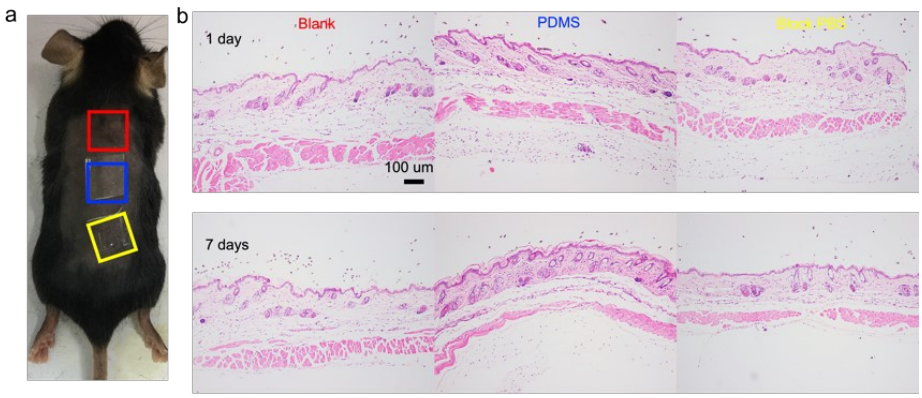

Figure S10. Biocompatibility test of PDMS and block PBS. a, PDMS is sutured on the skin of C57 rats. The block PBS can adhere to the skin. Red square-normal skin; Blue square-PDMS; Yellow square-block PBS. **b,** The skin samples under the block PBS and PDMS show no extra inflammatory cell infiltration in HE staining when compared with normal skin. Scale bar, 100 μm.

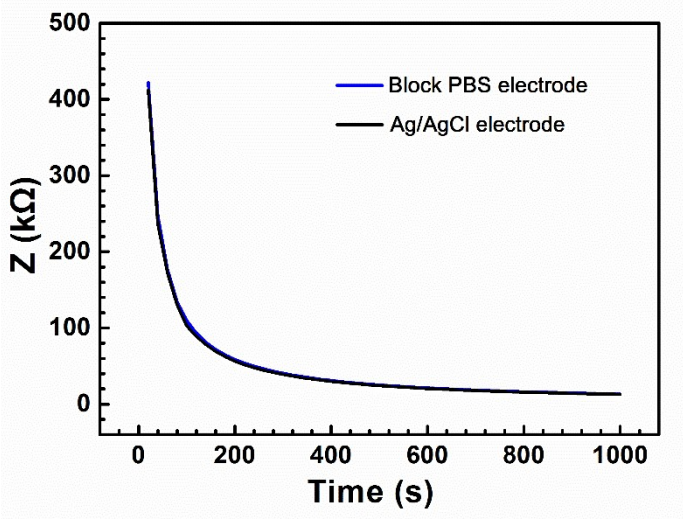

Figure S11. Contact impedance and impedance angle of the commercial and the block PBS-based electrodes.

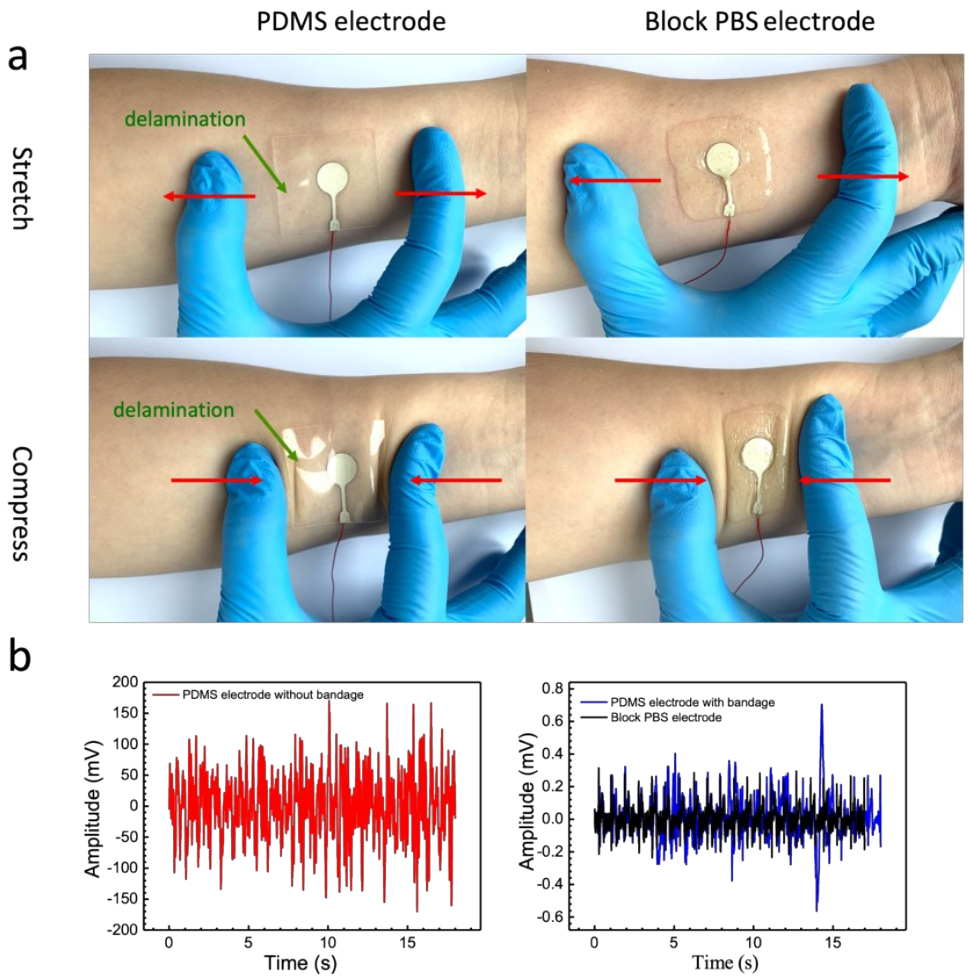

Figure S12. Performances and cardiac signals measured from the self-healable PBS ECG sensor and the PDMS sensor. a, Performances of the PDMS-based electrode vs. adhesive the block PBS-based electrode on skin during stretch and compression. No delamination is observed during deformation due to the high adhesion of block PBS-based electrode while PDMS-based one is easy to delaminate from the skin. b, Cardiac signals measured from the self-healable PBS ECG sensor (black) and the PDMS sensor with (blue) and without bandage (red). For PDMS-based electrode, only noise is observed without bandage. Even with bandage, its signals are not as stable as those pf the block PBS-based electrode.

Figure S13. Images of rats under ECG test conducted with block PBS electrodes in steady state.

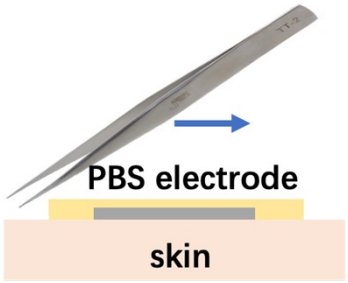

Figure S14. Schematic illustration of introducing damage on electrode during ECG test.

Table S1. M_n(kg/mol) and polydispersity Index (PDI) for three different v-PDMS precursors and synthesized block PDMS prepared with different v-PDMS precursors

Sample code	M_n (g/mol)	PDI
v-PDMS$_1$	4064	1.97
v-PDMS$_2$	8199	1.77
v-PDMS$_3$	12440	2.51
Block PDMS$_1$	44265	3.43
Block PDMS$_2$	46718	2.45
Block PDMS$_3$	65678	1.68

Table S2. Comparison of the performance of self-healing self-adhesive block PBS with the previously reported typical self-healing composites.

Materials	Mechanism	Self-healing condition	Healing time (min)	Healing efficiency (%)	Adhesion strength	Tensile strength(MPa)	Ref.
PDMS	Benzine boron ester bond	20 °C	600	70	No	7	[1]
		40 °C	360	97			
	Imine bond	rt	60	98.3	2.16 kpa	0.035	[2]
	Multiple hydrogen bonding	rt	720	98.3	No	1.7	[3]
	Multiple hydrogen bonding	Under water, -70 °C	5	98	No	5	[4]
		Under water, -20 °C	720	65			
		Under water, -20 °C	5760	84			
	Diels-Alder	80 °C	2880	73	No	0.35	[5]
	Multiple hydrogen bonding	rt	2880	78	No	1.6	[6]
	Multiple hydrogen bonding	55 °C	2880	93	No	1	[7]
	Zn coordination	25 °C	1440	98.9	No	3.2	[8]
	Multiple hydrogen bonding	rt	120	99	No	0.227	[9]
	Fe coordination	rt	2880	99	No	0.22	[10]
	Boroxine	Water, 70 °C	300	95	No	9.45	[11]
	Dynamic H-bonds and disulfide bond	rt	120	91	No	0.1	[12]
	Dynamic imine bonds	rt	1	99	700 kPa	0.11	[13]
	Physical entanglement	rt	30	97	No	0.1	[14]
	Hydrogen bonding and boronate ester bonding	**rt**	**0.5**	**100**	**356 Nm^{-1}**	**0.195**	**This work**
Hydrogels	Hydrogen bonding	rt	0.5	100	N/A	0.005	[15]
	Imine bond	rt	5	100	N/A	0.001	[16]
	Dynamic ionic interactions	rt	2	100	0.01	No	[17]
	Borate ester and imine bond	rt	45	98	0.0057	N/A	[18]
	Hydrophobic associations and	24 °C	20	100	0.028	No	[19]

	hydrogen bonding						
	Acylhydrazone bonds and micelle cross-linking	rt	1440	85	0.3	N/A	[20]
	Metal-ion coordinatio	rt	720	96.8	0.4	N/A	[21]
	Hydrogen bonding	rt	360	90.8	0.0357	12 kPa	[22]
	Urea bonds and hydrogen bonds	rt	720	91.8	0.36	N/A	[23]
	Hydrophobic association	rt	360	95	0.1043	N/A	[24]
	Hydrophobic interactions	50 °C	1440	100	0.202	N/A	[25]
Elastomers	Hydrogen bonding	25 °C	480	86	1.9	63 kPa	[26]
	Hydrogen bonding and molecular dynamics	rt	720	100	0.4	3488 Nm^{-1}	[27]
	Hydrogen bonding and imine bonds	rt	50	84	3	N/A	[28]
	Host-guest interactions	rt	10	readhere	8	N/A	[29]
	Multiple hydrogen bonding	rt	180	100	0.32	N/A	[30]
	Urea bonds and hydrogen bond	65 °C	180	99	1.5	N/A	[31]
	Disulfides	rt	120	90	6.76	N/A	[32]
	Hydrogen bonds	50 °C	180	90	1.66	N/A	[33]
	Boronic ester	50°C	960	95	2.9	N/A	[34]
	ion–dipole interactions	rt	1440	44	0.09	N/A	[35]
	Hydrogen bonds	rt	2880	88	0.5	N/A	[36]

Reference

1. H. Yu, Y. Feng, L. Gao, C. Chen, Z. Zhang and W. Feng, *Macromolecules*, 2020, **53**, 7161-7170.
2. B. Zhang, P. Zhang, H. Zhang, C. Yan, Z. Zheng, B. Wu and Y. Yu, *Macromol. Rapid Commun.*, 2017, **38**, 1700110.
3. K. Zhang, X. Shi, J. Chen, T. Xiong, B. Jiang and Y. Huang, *Chem. Eng. J.*, 2021, **412**, 128734.
4. M. Liu, P. Liu, G. Lu, Z. Xu and X. Yao, *Angew. Chem. Int. Ed.*, 2018, **130**, 11412-11416.
5. Q. Yan, L. Zhao, Q. Cheng, T. Zhang, B. Jiang, Y. Song and Y. Huang, *Ind. Eng. Chem. Res.*, 2019, **58**, 21504-21512.
6. J. Kang, D. Son, G. J. N. Wang, Y. Liu, J. Lopez, Y. Kim, J. Y. Oh, T. Katsumata, J. Mun and Y. Lee, *Adv. Mater.*, 2018, **30**, 1706846.
7. R. Du, Z. Xu, C. Zhu, Y. Jiang, H. Yan, H. C. Wu, O. Vardoulis, Y. Cai, X. Zhu and Z. Bao, *Adv. Funct. Mater.*, 2020, **30**, 1907139.
8. J.-C. Lai, X.-Y. Jia, D.-P. Wang, Y.-B. Deng, P. Zheng, C.-H. Li, J.-L. Zuo and Z. Bao, *Nat. Commun.*, 2019, **10**, 1-9.
9. P. F. Cao, B. Li, T. Hong, J. Townsend, Z. Qiang, K. Xing, K. D. Vogiatzis, Y. Wang, J. W. Mays and A. P. Sokolov, *Adv. Funct. Mater.*, 2018, **28**, 1800741.
10. C.-H. Li, C. Wang, C. Keplinger, J.-L. Zuo, L. Jin, Y. Sun, P. Zheng, Y. Cao, F. Lissel and C. Linder, *Nat. Chem.*, 2016, **8**, 618-624.
11. J. C. Lai, J. F. Mei, X. Y. Jia, C. H. Li, X. Z. You and Z. Bao, *Adv. Mater.*, 2016, **28**, 8277-8282.
12. H. Guo, Y. Han, W. Zhao, J. Yang and L. Zhang, *Nat. Commun.*, 2020, **11**, 1-9.
13. D.-P. Wang, Z.-H. Zhao, C.-H. Li and J.-L. Zuo, *Mater. Chem. Front.*, 2019, **3**, 1411-1421.
14. D.-P. Wang, Z.-H. Zhao and C.-H. Li, *ACS Appl. Mater. Interfaces*, 2021.
15. I. Jeon, J. Cui, W. R. Illeperuma, J. Aizenberg and J. J. Vlassak, *Adv. Mater.*, 2016, **28**, 4678-4683.
16. W. Huang, Y. Wang, Z. Huang, X. Wang, L. Chen, Y. Zhang and L. Zhang, *ACS Appl. Mater. Interfaces*, 2018, **10**, 41076-41088.
17. M. A. Darabi, A. Khosrozadeh, R. Mbeleck, Y. Liu, Q. Chang, J. Jiang, J. Cai, Q. Wang, G. Luo and M. Xing, *Adv. Mater.*, 2017, **29**, 1700533.
18. Y. Li, L. Yang, Y. Zeng, Y. Wu, Y. Wei and L. Tao, *Chem. Mater.*, 2019, **31**, 5576-5583.
19. M. P. Algi and O. Okay, *Eur. Polym. J.*, 2014, **59**, 113-121.
20. P. Wang, G. Deng, L. Zhou, Z. Li and Y. Chen, *ACS Macro Lett.*, 2017, **6**, 881-886.
21. S. Liu, K. Li, I. Hussain, O. Oderinde, F. Yao, J. Zhang and G. Fu, *Chemistry–A European Journal*, 2018, **24**, 6632-6638.

22. G. Ge, Y. Lu, X. Qu, W. Zhao, Y. Ren, W. Wang, Q. Wang, W. Huang and X. Dong, *ACS nano*, 2019, **14**, 218-228.
23. S. Liu, O. Oderinde, I. Hussain, F. Yao and G. Fu, *Polymer*, 2018, **144**, 111-120.
24. H. Chen, B. Hao, P. Ge and S. Chen, *Polym. Chem.*, 2020, **11**, 4741-4748.
25. G. Toleutay, E. Su, S. Kudaibergenov and O. Okay, *Colloid. Polym. Sci.*, 2020, **298**, 273-284.
26. Z. Xu, L. Chen, L. Lu, R. Du, W. Ma, Y. Cai, X. An, H. Wu, Q. Luo and Q. Xu, *Adv. Funct. Mater.*, 2021, **31**, 2006432.
27. Z. Zhang, N. Ghezawi, B. Li, S. Ge, S. Zhao, T. Saito, D. Hun and P. F. Cao, *Adv. Funct. Mater.*, 2021, **31**, 2006298.
28. Z. Jiang, B. Diggle, I. C. Shackleford and L. A. Connal, *Adv. Mater.*, 2019, **31**, 1904956.
29. J. Park, S. Murayama, M. Osaki, H. Yamaguchi, A. Harada, G. Matsuba and Y. Takashima, *Adv. Mater.*, 2020, **32**, 2002008.
30. R. Tamate, K. Hashimoto, T. Horii, M. Hirasawa, X. Li, M. Shibayama and M. Watanabe, *Adv. Mater.*, 2018, **30**, 1802792.
31. T. Li, Y. Wang, S. Li, X. Liu and J. Sun, *Adv. Mater.*, 2020, **32**, 2002706.
32. S. M. Kim, H. Jeon, S. H. Shin, S. A. Park, J. Jegal, S. Y. Hwang, D. X. Oh and J. Park, *Adv. Mater.*, 2018, **30**, 1705145.
33. J. A. Neal, D. Mozhdehi and Z. Guan, *J. Am. Chem. Soc.*, 2015, **137**, 4846-4850.
34. O. R. Cromwell, J. Chung and Z. Guan, *J. Am. Chem. Soc.*, 2015, **137**, 6492-6495.
35. Y. Cao, Y. J. Tan, S. Li, W. W. Lee, H. Guo, Y. Cai, C. Wang and B. C.-K. Tee, *Nature Electronics*, 2019, **2**, 75-82.
36. X. Yan, Z. Liu, Q. Zhang, J. Lopez, H. Wang, H.-C. Wu, S. Niu, H. Yan, S. Wang and T. Lei, *J. Am. Chem. Soc.*, 2018, **140**, 5280-5289.